Photoemission from small palladium clusters supported on various substrates

Shigemi Kohiki
Matsushita Technoresearch, Inc., Moriguchi, Osaka 570, Japan

Shigero Ikeda
Department of Chemistry, Faculty of Science, Osaka University, Toyonaka, Osaka 560, Japan
(Received 14 March 1986)

The core-electron binding energy obtained for small Pd clusters supported on various substrates is greater than that obtained for bulk Pd metal. The shifts of the core-electron binding energy and the core-valence-valence Auger-electron kinetic energy for small Pd clusters on the conductive amorphous carbon substrate are in good agreement with those calculated by the thermodynamic model using Miedema's semiempirical theory. Both experimentally and theoretically, the positive shift of the Pd core-electron binding energy with decreasing coverage is shown to be due to the photoemission initial-state effect. The shifts of the Pd core-electron binding energy with the coverage for small clusters on the semiconductive InSb and InP substrates are primarily due to the initial-state effect. The ratio of the photoemission initial-state-effect change to the photoemission final-state-effect change decreases with an increase of the polarizability of the substrate. The photoemission final-state effect predominantly arises from the positive shift of the Pd core-electron binding energy with decreasing coverage on the insulating SiO_2 and Al_2O_3 substrates. The changes in the terms of the extra-atomic relaxation energy for the Pd core hole and the potential energy of the Pd core electron differ for each substrate. The change in the extra-atomic relaxation energy for the Pd core hole varies with the change of the polarizability of the substrate. The change in the potential energy of the Pd core electron correlates with the difference in electronegativities of the substrate components.

I. INTRODUCTION

The electronic structure in small metal clusters supported on substrates is presently a subject of great interest in the transition of electronic states from the isolated atoms to the bulk metal. This interest has been motivated primarily by the tremendous technological importance of metal clusters, particularly in heterogeneous catalysis.[1-5]

The metal nuclei formed in the earliest stages of vapor deposition on well-characterized substrates are ideal systems to study by x-ray photoelectron spectroscopy (XPS). The metals studied to date include Cu, Ni,[6,7] Ag,[8,9] Au,[10-16] Pd,[6,7,13,17-21] and Pt.[17,18] The substrates used include C,[6-9,11-13,16-18,20] Al,[14] Cd,[13] In,[13] Sn,[13] Sb,[13] Te,[13] BN,[15] InP,[15] Al_2O_3,[11,13-15,19] SiO_2,[13,15,19,21] and alkali halides (NaCl, LiF, KCl).[10] Amorphous carbon is the most widely used substrate, and the noble metals and group-VIII metals are the most thoroughly studied metals.

Egelhoff and Tibbetts[6] reported that the core-level electron binding energies (BE's) of Cu, Ni, and Pd changed by larger amounts for amorphous carbon substrate than for crystalline carbon substrate.

It has been reported that the electron BE's for small metal clusters supported on poorly conducting substrates generally diminish with the increase of cluster atoms.[6-21] It is possible to consider two different origins for interpreting the BE shift. One of the origins is that the shift is a result of a size dependence of the initial-state electronic structure. The alternative one is that it is due to variations in final-state relaxation processes.

The interpretation of the BE change of the core level as a function of the cluster size has remained controversial. Citrin and Wertheim[22] suggested that the BE change is simply due to a shift in the reference level, while Mason[13] argued that the shift is caused by *sp-d* rehybridization.

In this paper small Pd clusters on various substrates were investigated. Pd is chosen because of its importance in the chemical industry and because considerably more information on this metal is available. The substrates discussed were amorphous carbon, InSb, InP, SiO_2, and Al_2O_3.

This paper presents the idea that the photoemission initial-state effect is responsible for the core-electron BE shift for small Pd clusters on the conductive amorphous carbon substrate and the photoemission final-state effect predominantly gives rise to the BE shifts for the small clusters supported on the insulative SiO_2 and Al_2O_3 substrates. In small Pd clusters supported on the semiconductive InSb and InP substrates, the photoemission initial-state effect primarily gives rise to the BE shifts. The ratio of the initial-state-effect change to the final-state-effect change differs for each substrate and decreases with an increase of the polarizability of the substrate. The change in the extra-atomic relaxation energy for the Pd core hole in small Pd clusters on the substrate correlates to the difference of the polarizability of the substrate and the Pd metal. The change in the core eigenvalue corresponding to the change of the potential energy of the Pd core electron for small clusters differs for each substrate and correlates to the difference in electronegativity of the substrate components. The "extra-ionic" energy affects

the Pd core-electron potential through the lattice potential energy. This result suggests that the heat of formation and the bond ionicity of the substrate can be estimated by the change in the photoemission initial-state effect of evaporated Pd.

II. PHOTOELECTRON AND AUGER ELECTRON ENERGY SHIFT

It is generally stated that the actual photon absorption process occurs nearly instantaneously ($\lesssim 10^{-17}$ s) and the hole switching occurs in a time very much less than 10^{-16} s. The localized screening response (10^{-16}–10^{-15} s) is very fast in contrast to the delocalized screening response (10^{-13}–10^{-12} s). Delocalized screening is accompanied with core-valence-valence (CVV) Auger transitions.[23]

The BE of a level j, $E_B(j)$, is the difference in the total energy of the system in its ground state and in the state with one electron missing in the orbital j. The $E_B(j)$ relative to the Fermi level is defined by the following equation:

$$E_B(j)=E_B^V(j)-\phi_{\rm sp} .$$

Here, E_B^V denotes the BE relative to the vacuum level and $\phi_{\rm sp}$ is the spectrometer work function. The $E_B(j)$ in solid phase relative to the Fermi level can be expressed[24] as

$$E_B(j)=-\varepsilon(j)-R^D(j)-\Delta E^{\rm corr}(j)-\Delta E^{\rm rel}(j) . \quad (1)$$

Here $-\varepsilon(j)$ is the term for orbital energy calculated by solving the Hartree-Fock (HF) equations by Koopmans's theorem, and $R^D(j)$ is the one-hole dynamic relaxation energy related to the photoemission process of Shirley.[25] Relaxation energy is the result of a flow of negative charge towards the hole created in the photoemission process in order to screen the suddenly appearing positive charge. The screening lowers the energy of the hole state left behind and therefore lowers the measured BE as well. The relaxation energy (R) can be partitioned into two terms: intra-atomic relaxation energy ($R_{\rm in}$) and extra-atomic relaxation energy ($R_{\rm ex}$). The former is constant for the core electrons of a given atom. The latter varies with changes in chemical and physical states.

Differential correlation $\Delta E^{\rm corr}(j)$ and relativistic $\Delta E^{\rm rel}(j)$ energies also should be contained in Eq. (1) because these terms are not included in the HF approximation.

According to Eq. (1), the photoelectron BE shift can be written as

$$\Delta E_B(j)=-\Delta\varepsilon(j)-\Delta R_{\rm ex}^D(j)-\Delta^2 E^{\rm corr}(j)-\Delta^2 E^{\rm rel}(j) . \quad (2)$$

Since $\Delta E^{\rm corr}(j)$ and $\Delta E^{\rm rel}(j)$ in Eq. (1) are very small, the terms $\Delta^2 E^{\rm corr}(j)$ and $\Delta^2 E^{\rm rel}(j)$ in Eq. (2) are disregarded in the following discussion. For most situations encountered in photoemission, the approximation

$$\Delta E_B(j)=-\Delta\varepsilon(j)-\Delta R_{\rm ex}^D(j) \quad (3)$$

is close enough to discuss the chemical shift.[26]

The kinetic energy (KE) relative to the Fermi level of an Auger electron emitted from a transition (jkl) is given[27] by

$$E_{\rm kin}(j,k,l;X)=E_B(j)-E_B(k)-E_B(l)-F(k,l;X)+R^S(k,l) , \quad (4)$$

where $E_B(j)$, $E_B(k)$, and $E_B(l)$ are the BE's of the core electrons j, k, and l, respectively. The processes of electron emission j and k include the dynamic relaxation, relativity, and electron correlation effects. The correction energy due to the presence of the k hole should be also considered in the process of electron emission l. $F(k,l;X)$ is the two-electron interaction energy, introduced by Asaad and Burhop,[28] describing the unscreened coupling of the two holes k and l in the multiplet final-state X. This term can be estimated by standard atomic multiplet coupling theory[29] and by tabulated F and G Slater integrals.[30] $R^S(k,l)$ is the static relaxation energy describing the polarization energy. Here,

$$R^S(k,l)=R^T(k,l)-R^D(k)-R^D(l) .$$

The difference between the total two-hole relaxation energy $R^T(k,l)$ and the two one-hole relaxation energies $R^D(k)$ and $R^D(l)$ is equal to the static relaxation energy. It gives the additional relaxation shift of the total energy associated with two localized holes relative to that of two isolated holes. If the two final-state holes have the same main quantum number n and angular momentum quantum number l, the total two-hole relaxation energy is four times the one-hole relaxation energy: $R^T(k,k)=4R^D(k)$. So, we have the result $R^S(k,k)=2R^D(k)$:[31,32] the static relaxation energy is twice the dynamic value.

According to Eq. (4), the Auger electron KE shift can be written as

$$\Delta E_{\rm kin}(j,k,l;X)=\Delta E_B(j)-\Delta E_B(k)-\Delta E_B(l)-\Delta F(k,l;X)+\Delta R_{\rm ex}^S(k,l) . \quad (5)$$

In this experiment we use Pd $3d_{5/2}$ photoelectrons and M_5VV Auger electrons. The two-hole interaction energy in the final-state valence band, $F(VV;X)$, is reasonably assumed to be independent of the number of Pd cluster atoms on each substrate. Therefore, $\Delta F(VV;X)$ is about zero. $\Delta F(k,l;X)$ in Eq. (5) can thus be omitted. Furthermore, identical final-state levels $k=l$ are involved in the M_5VV Auger process, and the relationship $\Delta R_{\rm ex}^S(VV)=2\Delta R_{\rm ex}^D(V)$ may be used as described above. In the simplest approximation, the change in extra-atomic relaxation energy can be derived from the combination of Pd $3d_{5/2}$ BE and M_5VV Auger KE referenced to the Fermi level. These quantities define the modified Auger parameter:

$$\alpha=E_B(3d_{5/2})+E_{\rm kin}(M_5VV) .$$

The difference in the modified Auger parameters for a given element in two different environments is twice the difference in dynamic extra-atomic relaxation energies,[32] $\Delta\alpha=2\Delta R_{\rm ex}^D(V)$. Then we have

$$\Delta E_{\rm kin}(M_5VV)=\Delta E_B(3d_{5/2})-2\Delta E_B(\bar{V})+2\Delta R_{\rm ex}^D(V) , \quad (6)$$

where $E_B(\bar{V})$ is the mean-valence-band electron BE.

If the assumption $\Delta R_{ex}^D(V)=\Delta R_{ex}^D(3d_{5/2})$, which has been found approximately for various levels,[33] is valid, Eqs. (3) and (6) yield the following result:

$$\Delta E_{kin}(M_5VV)=-\Delta\varepsilon(3d_{5/2})-2\Delta E_B(\bar{V})+\Delta R_{ex}^D(V)\ . \tag{7}$$

Here, $\Delta\varepsilon(3d_{5/2})$ denotes the shift of core eigenvalue corresponding to the difference between the potentials in the free atom and in the condensed phase. This term depends on the electronic structure in photoemission initial state. We define the change in this term as the change in the photoemission initial-state effect. $\Delta R_{ex}^D(V)$ describes the change of one-hole dynamic extra-atomic relaxation energy. The change in this term is defined as the change in the photoemission final-state effect.

A variation in the size of the work function for small metallic spheres has been reported.[34] The change of the work function can be explained by the following two contributions: an increase due to the attraction of the unit charge left behind by photoemission, and a reduction due to the weaker image potential of a sphere compared to that of a plane, giving a net increase of $5.40(\text{eV})/r(\text{Å})$ in the work function.[35] r is the radius of the metallic sphere. It is well known that the change in the work function does not affect the measured photoelectron BE and Auger electron KE relative to the Fermi level.[36] It is not necessary to consider the effect of size variation of the work function in this experiment.

Sample charging should bring the shifts which have the opposite sign and identical value of the Pd $3d_{5/2}$ BE and the Pd M_5VV KE at the same coverage. The value of shifts observed in the Pd $3d_{5/2}$ BE and the Pd M_5VV KE were different from each other at same coverage. It is obvious that sample charging cannot predict this difference.[19]

III. EXPERIMENTAL

The photoemission spectra measurements were made on a VG Scientific Ltd. ESCALAB-5 electron spectrometer using unmonochromatized Al$K\alpha$ radiation. The linewidth [full width at half maximum (FWHM)] for the Ag $3d_{5/2}$ photopeak was 1.15 eV. No attempt has been made to remove the instrumental broadening. The spectrometer was calibrated by utilizing the energy difference (233.0 eV) between Al $K\alpha$ and Mg $K\alpha$ radiation. Then, the core-level BE's of Pd, Ag, and Au foils were measured. The Pd $3d_{5/2}$, Ag $3d_{5/2}$, and Au $4f_{7/2}$ BE's were, respectively, 335.4, 368.3, and 84.0 eV relative to the Fermi level. The probable electron energy uncertainty amounts to 0.1 eV. The normal operating vacuum pressure was less than 3×10^{-8} Pa.

Pd M_5VV Auger electrons were excited by Al $K\alpha$ x rays. The Auger electron spectra were also recorded on the same instrument in the constant analyzer energy (CAE) mode.

The amorphous carbon film (500 Å thick), which was obtained by vapor deposition onto a polished nickel disk (8 mm in diameter), was sputtered with 7-keV Ar^+ ions in the sample preparation chamber of the spectrometer at room temperature. Ar^+ ion sputtering produced a clean surface on the substrate. Spectra of the valence-band (VB), Pd $3d$, Pd M_5VV, Ar $2p$, O $1s$, and C $1s$ regions were recorded to monitor the condition of the substrate. No oxygen contamination could be detected. The atomic concentration of implanted Ar was 2.9%.

The single crystalline InSb and InP surfaces were sputtered with 7-keV Ar^+ ions in the sample preparation chamber of the spectrometer at room temperature. The sputtered substrate was not annealed to maintain the amorphous surface. Ar^+ ion sputtering produced a clean surface of the substrate. Spectra of the valence-band (VB), In $3d$, Sb $3d$, P $2p$, Pd $3d$, Pd M_5VV, Ar $2p$, O $1s$, and C $1s$ regions were recorded to monitor the condition of the substrate. No carbon and oxygen contamination could be detected. The atomic concentration of implanted Ar was 2.6% for InSb and 1.8% for InP.

The composition of sputtered substrate surfaces before Pd deposition was measured by varying the photoelectron take off angle ($\theta=10°$, 25°, 35°, 50°, 90°). The effect of preferential sputtering was negligible in this experiment. The effect of preferential sputtering reported is serious for relatively low energy ($\lesssim$1.5 keV) and for small atomic number (He,Ne) primary ion. In this experiment relatively high energy (7 keV) and a heavier (Ar) primary ion was used for sputtering.

The Pd was deposited by vapor deposition in the sample preparation chamber at room temperature. The sample was transferred between the analyzer chamber and the preparation chamber under a vacuum below 3×10^{-8} Pa. The coverage of the Pd was determined from the Pd $3d_{5/2}$ peak intensity.[15]

In the case of carbon substrate, BE's were referred to the C $1s$ line of the substrate, which had a value of 284.6 eV. This value was consistent with a zero BE for the Fermi edge at high coverage. In the case of semiconductor substrates, BE's were referred to the $2p_{3/2}$ line of the Ar implanted into the substrates, which had a value of 242.3 eV.[37]

A microcomputer was used for data acquisition and data processing. Determination of the core-level peak positions and spectral intensities (peak areas) was accomplished after subtracting a background noise by smoothing the experimental data.

The relationship between the coverage and the cluster size was not determined directly in this experiment. Hamilton and Logel[38] have reported the variation in cluster-size distribution with Pd coverage on amorphous carbon substrate. They demonstrated that the deposited Pd atoms are predominantly adsorbed as isolated adatoms at coverage of less than $\frac{1}{4}$ monolayer and that at higher coverages clusters grow by random adsorption of metal atoms. Takasu *et al.*[21] studied Pd on SiO_2. The bond ionicity of SiO_2 is known to be 0.61.[39] They showed that only a part of the incident metal (probably 20% at 7×10^{14} atoms cm^{-2}) is present in the particles (average particle size 1.6 nm) and at coverage 7×10^{15} atoms cm^{-2} the average particle size is 4.2 nm. A rapid increase in the fractional area covered occurs on ionically bonded SiO_2 substrate.

IV. RESULTS AND DISCUSSION

The degree of cluster-substrate interaction for clusters of Pd evaporated on poorly conducting substrates can be divided into two categories: (i) substrates with localized p orbitals with BE's overlapping that of the cluster d orbital, and (ii) substrates without such orbitals. The former is considered strongly interacting, whereas the latter type is only weakly interacting.

Table I shows the p-electron BE's of the substrate components. The p-d interaction will be repulsive and will increase as the energy separation decreases. It is expected that the semiconductor (InSb and InP) substrates are strongly interacting. Semiconductor substrate components have a density of state near the Fermi level ($E_B \lesssim 2$ eV). In III-V compounds, the most intense features are the d-levels peaks in the cations centered around 15-eV BE and those of the anions around 35 eV. Additional structure typically from 5 to 10% as intense as the d-level peaks is observed in the $E_B = 0$–4 eV region. This structure is attributed in each case to the valence bonds formed from the outermost atomic s and p orbitals of the two constituent elements.[40]

It is well known that Pd particles supported on carbon sinter readily[41] in comparison with Pd on silica. This should reflect the weak interaction between the Pd clusters and the carbon substrate. The C $2p$ BE is 6 eV relative to the Fermi level. The weak cluster-substrate interaction is perhaps due to the low density of states in the semimetallic carbon substrate. The amorphous carbon substrate is conductive while the SiO_2 is a good insulator. This can have an influence on the screening of the holes created by the photoemission. There is rapid transfer of an electron to the cluster from the carbon substrate. Since the interaction between the Pd clusters and the carbon substrate is rather weak, we expect that the contribution to the linewidth broadening due to a distribution of chemical inequivalent sites should be negligible. It is very convenient for us to compare the experimentally observed BE shifts to the theoretically calculated BE shifts in the Pd-C system.

In the insulator substrates (SiO_2 and Al_2O_3),[19] the $2p$ levels of the cations range from 3 to 5 eV and the O $2p$ BE is 7 eV relative to the Fermi level. The radii of the Si, Al, and O ions are 0.4, 0.5, and 1.4 Å, respectively. Both the physical and electronic structures of SiO_2 and Al_2O_3 are dominated by the O ion. The density of states near the Fermi level in the semiconductor substrates is relatively higher than that in the insulator substrates. This relatively high density of states near the Fermi level facilitates charge transfer and hence neutralization of the positive charge in the cluster in final state. On insulating substrates a hole state created in the cluster cannot be easily neutralized via fast electronic relaxation. There are no itinerant electron states through which electronic charge could be readily transferred. The available mechanisms for screening the incremental positive charge are relaxation of neighboring ions and polarization of the electronic charge on those ions. The former is too slow to affect the active electron's BE, therefore only the latter is effective.

TABLE I. The BE's of p levels of the substrate components. BE relative to the Fermi level is given in eV.

Energy (eV)	Orbitals
1	In $5p^1$
2	Sb $5p^3$
3	Si $3p^2$
5	Al $3p^1$
6	C $2p^2$
7	O $2p^4$
10	P $3p^3$

The detailed mechanism of extra-atomic relaxation differs between ionic, covalent, and metallic materials. A metal has itinerant electron states. The extra-atomic relaxation energy in metals is larger than that observed in insulators. In covalently bonded semiconductors and semimetals extra-atomic relaxation can take place effectively through the bonds which are polarized and electronic charge shifts towards the cation atom, screening the positive hole. In an ionic solid, extra-atomic relaxation cannot easily take place via electronic relaxation.[42] Fadley *et al.*[43] pointed out that electrons on neighboring ions will respond to the sudden creation of a positive charge during photoemission by moving away from their equilibrium positions so as to change the electrostatic potential at the site of the ionized atom. The extra-atomic relaxation energy observed in an ionic solid is smaller than that observed in a covalent solid.

In the photoemission final state, the hole state of the Pd core level should be screened by the valence electrons of the Pd cluster and the conduction electrons of the substrate. This relaxation shift depends on the relative magnitude of the polarizability of the substrate and the Pd metal. It is expected that the polarization energy of the substrate, screening the core-hole state in the cluster, is small for small Pd clusters on insulator substrates, in contrast with the case of semiconductor substrates.

The results obtained in the conductive carbon substrate experiment are shown in Figs. 1–3. Figure 1 shows the Pd $3d_{5/2}$ BE versus the Pd coverage. The Pd $3d_{5/2}$ BE increases by 1.1 eV with decreasing coverage from 4×10^{15} to 8×10^{13} atoms cm^{-2} and is almost constant in cover-

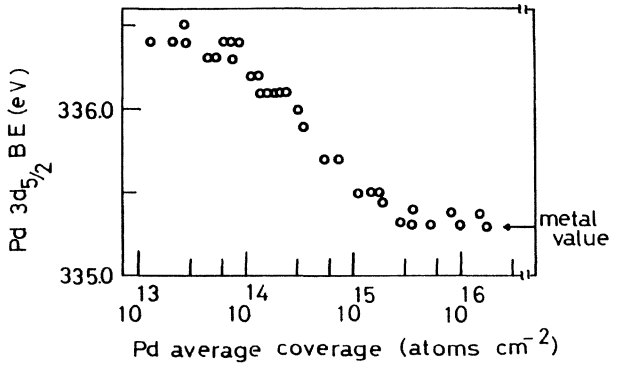

FIG. 1. Coverage dependence of the Pd $3d_{5/2}$ electron binding energy (BE) of the Pd clusters on the C substrate.

ages below 8×10^{13} atoms cm^{-2}. The Pd $3d_{5/2}$ BE in coverages of more than 4×10^{15} atoms cm^{-2} is constant and identical to that obtained for bulk Pd metal.

Figure 2 shows the Pd M_5VV Auger KE versus the Pd coverage. The Pd M_5VV Auger KE shifts by $+1.3$ eV with increasing coverage from 8×10^{13} to 4×10^{15} atoms cm^{-2}. The Pd Auger KE is almost constant both in regions less than 8×10^{13} and more than 4×10^{15} atoms cm^{-2}. The Pd Auger KE in coverages greater than 4×10^{15} atoms cm^{-2} is identical to that obtained for bulk metal.

Figure 3 shows the modified Auger parameter versus the Pd coverage. α is almost constant at coverages below 1×10^{15} atoms cm^{-2}. Therefore, the extra-atomic relaxation energy did not change. In the higher-coverage region [$(1-4)\times10^{15}$ atoms cm^{-2}], α increases by 0.2 eV with increasing coverage. In this coverage region the change in the dynamic extra-atomic relaxation energy is equal to 0.1 eV.

In region I (coverage less than $\approx8\times10^{13}$ atoms cm^{-2}) $\Delta E_{\rm kin}(M_5VV)=0$ eV, $\Delta E_B(3d_{5/2})=0$ eV, and $\Delta R_{\rm ex}^D(V)=0$ eV. Therefore, $\Delta E_B(\bar{V})=0$ eV.

In region II [coverage $(8\times10^{13})-(1\times10^{15})$ atoms cm^{-2}] $\Delta E_{\rm kin}(M_5VV)=+0.8$ eV, $\Delta_B(3d_{5/2})=-0.85$ eV, and $\Delta R_{\rm ex}^D(V)=0$ eV. $\Delta E_B(\bar{V})$ is equal to -0.83 eV.

In region III [coverage $(1\times10^{15})-(4\times10^{15})$ atoms cm^{-2}] $\Delta E_{\rm kin}(M_5VV)=+0.5$ eV, $\Delta E_B(3d_{5/2})=-0.25$ eV, and $\Delta R_{\rm ex}^D(V)=+0.1$ eV. $\Delta E_B(\bar{V})$ is equal to -0.28 eV.

In region IV (coverage more than $\approx4\times10^{15}$ atoms cm^{-2}) $\Delta E_{\rm kin}(M_5VV)=0$ eV, $\Delta E_B(3d_{5/2})=0$ eV, and $\Delta R_{\rm ex}^D(V)=0$ eV. $\Delta E_B(\bar{V})$ is equal to 0 eV.

$\Delta\varepsilon(3d_{5/2})$ can be obtained from Eq. (7). In Table II $\Delta E_{\rm kin}(M_5VV)$, $\Delta E_B(3d_{5/2})$, $\Delta R_{\rm ex}^D(V)$, and $\Delta\varepsilon(3d_{5/2})$ are listed. In the lower-coverage regions (I and II), the -0.85-eV shift for the Pd $3d_{5/2}$ BE is ascribed to the change ($+0.85$ eV) in the initial-state effect $\Delta\varepsilon(3d_{5/2})$. In the higher-coverage regions (III and IV), the sum of the change in the initial-state effect and the change in the final-state effect corresponds to the change in the Pd $3d_{5/2}$ BE.

At low coverage the $+1.1$-eV shift of the Pd $3d_{5/2}$ BE and the -1.3 eV shift of the Pd M_5VV Auger KE relative to the bulk Pd are observed in evaporated Pd on the amorphous carbon substrate. The $+1.1$-eV shift for the Pd $3d_{5/2}$ BE is ascribed to the change ($+1.0$ eV) of the initial-state effect.

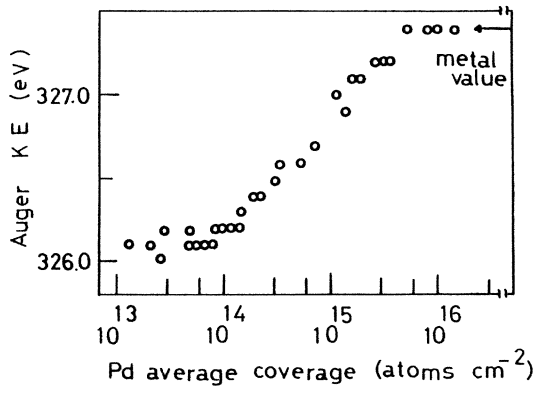

FIG. 2. Coverage dependence of the Pd M_5VV Auger electron kinetic energy (KE) of the Pd clusters on the C substrate.

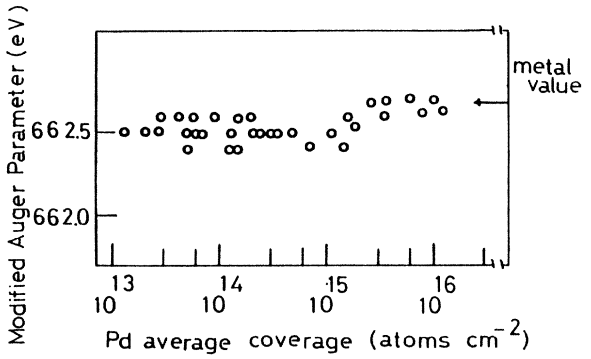

FIG. 3. Coverage dependence of the modified Auger parameter (α) of the Pd clusters on the C substrate.

Johansson and Mårtensson[44] developed a method for calculating the core-level electron BE shift between the free atom and the condensed atom in its metallic state. The thermodynamic model assumes that the core-ionized atom in the metal is screened completely and the final-state valence electron distribution can be substituted by that of an impurity atom with charge $(Z+1)$ in the original Z-atomic metal. The final state is reached from the initial state by means of a Born-Haber cycle, in which the energy of solution for a $Z+1$ impurity ion (of charge $+1$) in a host metal Z, gives a major contribution to the core-level BE shift. The core-level shift $(\Delta E_B)_{\rm calc}$ of an atom A when the atom A is removed from the pure metal and dissolved into host B can be written as[45]

$$(\Delta E_B^b)_{\rm calc}=E(A;B)+E(A+1;A)-E(A+1;B)\ , \qquad (8)$$

where the superscript b refers to the atom being dissolved in the bulk. Terms of the form $E(A;B)$ represent the solution energy of atom A in host B, and $A+1$ refers to the element with an atomic number one greater than that of A. The first term $E(A;B)$ represents the change in the initial-state energy of atom A upon solution in B. The remaining two terms, $E(A+1;A)$ and $E(A+1;B)$, represent the difference in final-state energies in hosts A and B.

The solution energy of the Pd atom into carbon was calculated by using the Miedema's semiempirical theory.[46] The values of E(Pd;C), E(Ag;Pd), and E(Ag:C) are 1.98, 0.23, and 0.77 eV, respectively. In this system we obtain a $+1.98$-eV shift due to the initial state, a -0.54-eV shift due to the final state, and a 1.44-eV shift as $(\Delta E_B^b)_{\rm calc}$. It is necessary to correct the surface-to-bulk shift of Pd for comparing the calculated bulk shift to the experimental value. The surface-to-bulk shift of Pd reported[22] was 0.3 eV. The corrected value is 1.14 eV, which is in good agreement with 1.1 eV of experimental shift. The experimental shifts due to the initial state and final state is $+1.0$ and $+0.1$ eV, respectively. Both experimentally and theoretically, it was shown that the $+1.1$-eV shift of

TABLE II. Changes of Auger electron kinetic energy, core-electron binding energy, photoemission final-state effect, and photoemission initial-state effect for Pd clusters on the carbon substrate with increasing coverage. Energies are given in eV.

Coverage (atoms/cm^2)	$\Delta E_{\rm kin}(M_5VV)$	$\Delta E_B(3d_{5/2})$	$\Delta R_{\rm ex}^D(V)$	$\Delta\varepsilon(3d_{5/2})$
Region I ($\lesssim 8\times10^{13}$)	0	0	0	0
Region II [(8×10^{13})–(1×10^{15})]	+0.8	−0.85	0	+0.85
Region III [(1×10^{15})–(4×10^{15})]	+0.5	−0.25	+0.1	+0.15
Region IV ($\gtrsim 4\times10^{15}$)	0	0	0	0

Pd $3d_{5/2}$ BE in evaporated Pd on amorphous carbon substrate is primarily due to the initial-state effect.

The change of Auger KE of the (jkl) process is analyzed in terms of the change of the one-hole state energy and the change of the two-hole state energy[31,47] as follows:

$$\Delta E_{\rm kin}(j,k,l)=\Delta E_B(j)-\Delta E_B(k,l)\ .$$

$E_B(k,l)$ is the energy required to create two holes on the same atom. We can derive an approximation similar to Eq. (8) to obtain the change of the two-hole state energy $\Delta E_B(k,l)$:[48]

$$(\Delta E_B^b)_{\rm calc}(k,l)=E(A;B)+E(A+2;A)-E(A+2;B)\ , \tag{9}$$

where $A+2$ is the $(Z+2)$ element relative to A.

The values of E(Cd;Pd) and E(Cd;C) are 1.42 and 0.45 eV, respectively. In evaporated Pd on the carbon substrate we have a 2.95-eV shift of the two-hole state energy $(\Delta E_B^b)_{\rm calc}(k,l)$.

We turn to the discussion of the Auger KE shift. We have a −1.51-eV shift for $(\Delta E_{\rm kin}^b)_{\rm calc}(j,k,l)$ because the change of the one-hole state energy $(\Delta E_B^b)_{\rm calc}(j)$ is 1.44 eV. After the correction of surface-to-bulk shift (0.3 eV), we obtain the calculated Auger KE shift (−1.21 eV). This value is in agreement with the experimental shift (−1.3 eV) within the experimental energy uncertainty (0.1 eV).

Mason[13] reported a 2.2-eV Auger shift for evaporated Pd on amorphous carbon substrate. This value is too large compared to the shift observed in this experiment and the calculated shift obtained from the thermodynamical model using Miedema's semiempirical theory. It is necessary to consider the change of the work function in the Mason's electron-excited Auger measurement to interpret the discrepancy. In the electron-excited Auger measurement the electron energy reference level is taken to the vacuum level. The work function varies with the change of cluster size as described in Sec. II. In small clusters, the work function increases. For the sphere radius $R\sim5$ Å, it amounts to ~1 eV. The increase of work function lowers the KE of the emitted electrons referenced to the vacuum level. However, the emitted electron KE referenced to the Fermi level is not altered by the change of work function with cluster size change.

Cheung[18] reported a reduction in the line-shape asymmetry, a broadening in the linewidth, and a shift of the core level toward the higher BE in evaporated Pd on the carbon substrate. The substrate is a different form of carbon from this experiment. The shift of core-level BE reported by Cheung is +0.8 eV, which is smaller than that obtained in this experiment. However, the paper by Cheung presents essentially identical results for the BE shift of evaporated Pd on the carbon substrate. The shift predominantly arises from an initial-state effect for small Pd clusters. The changes in the linewidth and line asymmetry can be interpreted in terms of the final-state effects—the changes in the response of the valence elec-

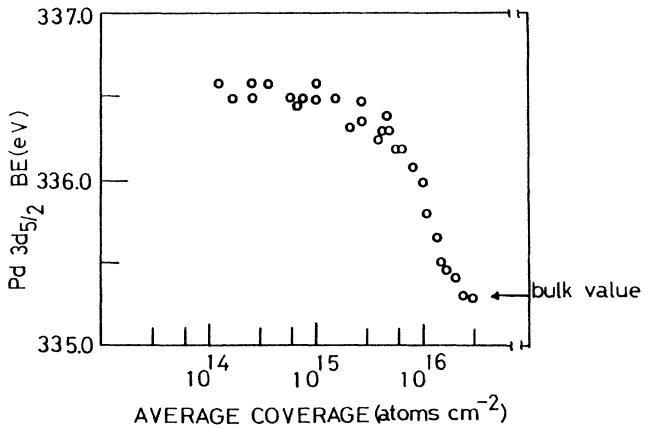

FIG. 4. Coverage dependence of the Pd $3d_{5/2}$ electron binding energy (BE) of the Pd clusters on the InSb substrate.

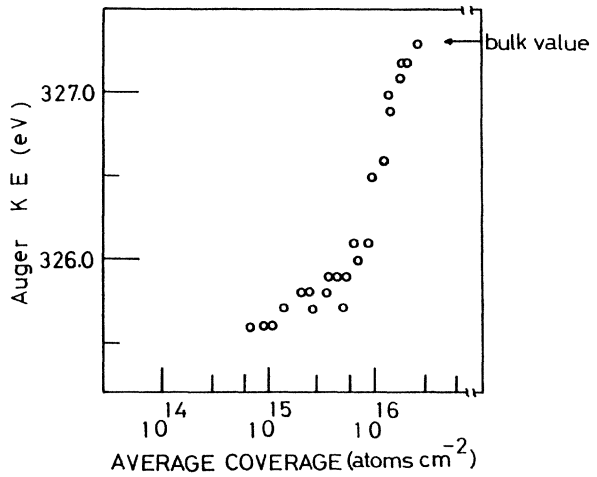

FIG. 5. Coverage dependence of the Pd M_5VV Auger electron kinetic energy (KE) of the Pd clusters on the InSb substrate.

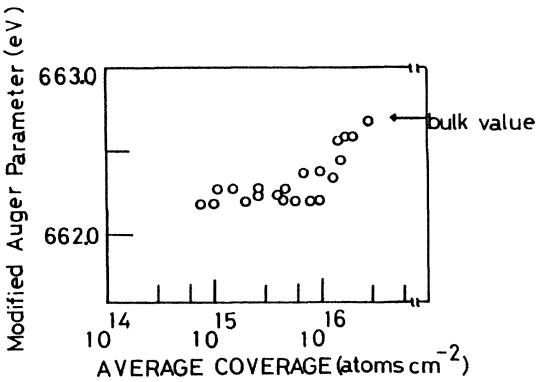

FIG. 6. Coverage dependence of the modified Auger parameter (α) of the Pd clusters on the InSb substrate.

trons to the core hole as a function of the cluster size.

The results obtained in the semiconductive InSb substrate experiment are shown in Figs. 4–6.

Figure 4 shows the Pd $3d_{5/2}$ BE versus the Pd coverage. The Pd $3d_{5/2}$ BE is constant in the low-coverage region (less than $\approx 1\times 10^{15}$ atoms cm^{-2}). In the region of intermediate coverage [$(1-8)\times 10^{15}$ atoms cm^{-2}], the Pd $3d_{5/2}$ BE decreased by 0.4 eV with increasing coverage. The Pd $3d_{5/2}$ BE for Pd clusters in the high-coverage region (more than $\approx 8\times 10^{15}$ and less than $\approx 3\times 10^{16}$ atoms cm^{-2}) decreased by 0.8 eV with increasing coverage.

Figure 5 shows the Pd M_5VV Auger KE versus the Pd coverage. The Pd M_5VV Auger KE shifts by $+0.50$ eV in the intermediate- and $+1.2$ eV in the high-coverage regions with the increase of coverage.

Figure 6 shows the modified Auger parameter versus the Pd coverage. α is almost constant at coverages below $\approx 8\times 10^{15}$ atoms cm^{-2}. Therefore, the dynamic extra-atomic relaxation energy did not change. In the higher-coverage region (Pd $\gtrsim 8\times 10^{15}$ atoms cm^{-2}), α increases by 0.5 eV with the increase of coverage. In this coverage region the change in the dynamic extra-atomic relaxation energy $\Delta R^D_{ex}(V)$ amounts to 0.25 eV.

In region II [Pd $\approx (1-8)\times 10^{15}$ atoms cm^{-2}], $\Delta E_{kin}(M_5VV)$ is $+0.50$ eV, $\Delta E_B(3d_{5/2})$ is -0.4 eV, and $\Delta\alpha$ is $+0.1$ eV with increasing coverage. From Eq. (7), $\Delta E_B(\bar{V})$ amounts to -0.4 eV.

In region III (Pd $\gtrsim 8\times 10^{15}$ atoms cm^{-2}), $\Delta E_{kin}(M_5VV)$ is $+1.2$ eV, $\Delta E_B(3d_{5/2})$ is -0.8 eV, and $\Delta\alpha$ is $+0.4$ eV with increasing coverage. $\Delta E_B(\bar{V})$ amounts to -0.8 eV.

$\Delta\varepsilon(3d_{5/2})$ can be obtained from Eq. (7). In Table III $\Delta E_{kin}(M_5VV)$, $\Delta E_B(3d_{5/2})$, $\Delta R^D_{ex}(V)$, and $\Delta\varepsilon(3d_{5/2})$ are listed. In region II the -0.4-eV shift for the Pd $3d_{5/2}$ BE is primarily ascribed to the change ($+0.35$ eV) in the initial-state-effect, $\Delta\varepsilon(3d_{5/2})$. In region III, the sum of initial-state-effect change and the final-state-effect change is in agreement with the change in the Pd $3d_{5/2}$ BE.

Similar changes of $E_{kin}(M_5VV)$, $E_B(3d_{5/2})$, $R^D_{ex}(V)$, and $\varepsilon(3d_{5/2})$ are obtained in small Pd clusters on the InP substrate. In Table IV, $\Delta E_{kin}(M_5VV)$, $\Delta E_B(3d_{5/2})$, $\Delta R^D_{ex}(V)$, and $\Delta\varepsilon(3d_{5/2})$ of Pd are listed. $\Delta\varepsilon(3d_{5/2})$ are identical for InSb and InP substrates. $\Delta R^D_{ex}(V)$ for the InP substrate is greater than that for the InSb substrate. Here we define the ratio of the photoemission initial-state-effect change to the photoemission final-state-effect change, $E_{i/f}$, as the ratio of $\Delta\varepsilon(3d_{5/2})$ to $\Delta R^D_{ex}(V)$. The value of $E_{i/f}$ for InSb substrate is greater than that for InP substrate. The change of final-state effect increases with the increase of the band gap and Schottky barrier height of the semiconductor as shown in Table V.

The bond ionicity (f_i) of InSb is 0.32 and that of InP is 0.42.[49] These are covalent semiconductors. Mead and Spitzer[50] have shown that for covalent semiconductors, the energies of Schottky barrier, formed by intimate contact between a metal and a semiconductor, were relatively independent of the particular metal, and the value of the barrier for electrons was approximately two-thirds of the band-gap energy.

Mead[51] and Kurtin *et al.*[52] demonstrated a distinctly different variation of the barrier behavior on ionic insulators as contrasted with covalent semiconductors. For the ionic insulator, the barrier energies are found to vary strongly with the particular metal. For covalent semiconductors (i.e., InSb, InP), Mead[51] argued that the lattice disruption at the surface was large, in contrast to ionic insulators (i.e., SiO_2, Al_2O_3), where crystal bonding is more Coulombic and less disruption of the lattice potential near the surface is expected, resulting in lower density of surface states.

At the metal-semiconductor interface, electrons flow from the semiconductor to the metal after contact. The barrier height depends on the difference in the work function in simple model. When we treat real Schottky barriers, we should consider the role of semiconductor surface states leading to band bending at the semiconductor-vacuum interface. The Schottky barrier height is expressed as

$$\phi_B = \phi_m - x_{sc} - \Delta x \ .$$

Here ϕ_B is the Schottky barrier height, ϕ_m is the work function of the metal, x_{sc} is the electron affinity of the semiconductor, and ΔX is dipole potential, which depends on the position of surface states within the band gap. The dipole layer is a capacitive layer with a negative charge on the metal side and a positive charge on the semiconductor side. It is well known that the Fermi level was pinned at the center of the band gap in covalent bonded semiconductor surfaces. So, we can use following approximate equation in the discussion of Schottky barrier height:

$$\phi_B = \phi_m - x_{sc} \ .$$

In the photoemission final state, electronic relaxation takes place through the Schottky barrier to small Pd clusters from the semiconductor substrates. So, the extra-atomic relaxation energy change observed in Pd depends on the polarizability of the substrates $(\epsilon_\infty - 1)/(\epsilon_\infty + 2)$.

The shifts for Pd $3d_{5/2}$ BE in small Pd clusters on SiO_2 and Al_2O_3 substrates, listed in Table VI, are predominantly ascribed to the change of photoemission final-state effect.[19] Of course, the sum of the change in the photoemission initial-state effect and the change in the photoemission final-state effect corresponds to the change of Pd

TABLE III. Changes of Auger electron kinetic energy, core-electron binding energy, photoemission final-state effect, and photoemission initial-state effect for Pd clusters on the InSb substrate with increasing coverage. Energies are given in eV.

Coverage (atoms/cm^2)	$\Delta E_{\rm kin}(M_5VV)$	$\Delta E_B(3d_{5/2})$	$\Delta R_{\rm ex}^D(V)$	$\Delta\varepsilon(3d_{5/2})$
Region I ($\lesssim 1\times10^{15}$)		0		
Region II [$\approx(1-8)\times10^{15}$]	+0.5	−0.4	+0.05	+0.35
Region III ($\gtrsim 8\times10^{15}$)	+1.2	−0.8	+0.2	+0.6

TABLE IV. Changes of Auger electron kinetic energy, core-electron binding energy, photoemission final-state effect, and photoemission initial-state effect for Pd clusters on the semiconductor substrates with increasing coverage. Energies are given in eV.

Substrate	$\Delta E_{\rm kin}(M_5VV)$	$\Delta E_B(3d_{5/2})$	$\Delta R_{\rm ex}^D(V)$	$\Delta\varepsilon(3d_{5/2})$
InSb	+1.7	−1.2	+0.25	+0.95
InP	+2.3	−1.4	+0.45	+0.95

TABLE V. Ratios of the changes in the photoemission initial-state and final-state effects, band gaps, electron affinities, Schottky barrier heights, and polarizabilities of the substrates. Energies are given in eV.

Substrate	$E_{i/f}$	E_g(300 K)	$x_{\rm sc}$	ϕ_B[a]	$(\epsilon_\infty-1)/(\epsilon_\infty+2)$[b]
InSb	3.8	0.18	4.6	0.2	0.83
InP	2.1	1.4	4.4	0.4	0.74

[a]$\phi_B=\phi_m-x_{\rm sc}$ and $\phi_{\rm Pd}=4.8$ eV.
[b]Reference 49. ϵ_∞ is the dynamic dielectric constant.

TABLE VI. Changes of Auger electron kinetic energy, core-level-electron binding energy, photoemission final-state effect, and photoemission initial-state effect in small Pd clusters on the substrates with increasing coverage (Ref. 19). Energies are given in eV.

Substrate	$\Delta E_{\rm kin}(M_5VV)$	$\Delta E_B(3d_{5/2})$	$\Delta R_{\rm ex}^D(V)$	$\Delta\varepsilon(3d_{5/2})$
SiO_2	+3.9	−1.7	+1.1	+0.6
Al_2O_3	+2.6	−1.2	+0.7	+0.5

TABLE VII. Correlation of the ratio of the initial-state effect change to the final-state effect change and the modified Auger parameter change with the polarizability of the substrates (Ref. 19).

Substrate	$E_{i/f}$	$\Delta\alpha$	$(\epsilon_\infty-1)/(\epsilon_\infty+2)$	Bulk polarizability[a] (Å^3)
SiO_2	0.55	2.2	0.32	4.3
Al_2O_3	0.71	1.4	0.79	3.0

[a]Reference 55.

$3d_{5/2}$ BE with each substrate. This result is clearly consistent with that of Vedrine *et al.*[3] They reported that a 1.4-eV shift for the Pd $3d$ line of atomically dispersed Pd in type-Y zeolites was assigned to smaller electron relaxation energy.

In photoemission final state, the hole state of the Pd core level in the cluster should be screened by the valence electrons of the Pd clusters and the conduction electrons of the substrates. This relaxation shift depends on the relative magnitude of the polarizability of the substrate and the Pd metal.

In ionic insulators the effective mechanism for screening the incremental positive charge is polarization of the electronic charge on neighboring ions. The BE will be reduced by a corresponding polarization energy ($E_{\rm pol}$). The polarization contribution must therefore be regarded as a form of static extra-atomic relaxation.

The one-hole relaxation cannot be measured directly whereas that due to Auger ionization can. The change of the modified Auger parameter of Pd is a measure of $E_{\rm pol}$ due to the substrate.

The term of $(\epsilon_\infty-1)/(\epsilon_\infty+2)$ is the measure of the polarizability of the substrate. The bulk polarizability of the substrate is calculated by the Clausius-Mossoti relationship. The value of $E_{i/f}$, $\Delta\alpha$, $(\epsilon_\infty-1)/(\epsilon_\infty+2)$, and bulk polarizability are listed in Table VII. $E_{i/f}$ for the Al_2O_3 substrate is greater than that for the SiO_2 substrate. $\Delta\alpha$ observed for the Al_2O_3 substrate is smaller than that observed for the SiO_2 substrate. The role of the photoemission final-state-effect change in Pd $3d_{5/2}$ BE change of small Pd cluster on substrates increases with the increase of the bulk polarizability of the substrate.

The difference in the change of the modified Auger parameter between the Al_2O_3 substrate and the SiO_2 substrate may suggest that the one-hole extra-atomic relaxation energy for SiO_2 is smaller than that for Al_2O_3. The screening should be weaker for clusters evaporated onto a more insulating, highly polarizable substrate.

Pd clusters on Al_2O_3 and SiO_2 substrates, investigated in Ref. 19, represent a close facsimile of the important small-metal particle catalysis.[1–5] In Ref. 19 it has been shown that small Pd clusters contain fewer d electrons. The result may suggest a correlation between the density of empty d electron states and the variation in catalytic activity with cluster size.

In the point-charge approximation the shift of the Pd core eigenvalue is given by the following equation:[53]

$$\Delta\varepsilon = kq + \Delta V \ .$$

In this experiment, q is the charge at the photoionized Pd atom, V is the electrostatic potential at the Pd nucleus created by the charges of the substrates. In practice, the term of kq will remain constant for each substrate. The change in $\Delta\varepsilon$ with the substrate will relate to difference in potential ΔV between the substrates.

Figure 7 shows the change in the photoemission initial-state effect $\Delta\varepsilon(3d_{5/2})$ versus the potential energy of the substrates. The change in the term of the core eigenvalue corresponds to the shift of the potential energy of the Pd core electron from bulk Pd metal to Pd atom dissolved into the matrix of the substrate. The change in the potential energy of the Pd core electron for small Pd clusters differs for each substrate and correlates to the difference in electronegativity of the substrate components.

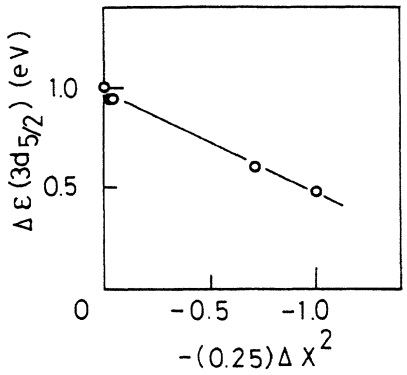

FIG. 7. The change in the term of Pd core eigenvalue versus the potential energy of the substrates. The values of ΔX for the C—C, In—Sb, In—P, Si—O, and Al—O bonds are 0, 0.2, 0.4, 1.7, and 2.0, respectively. The potential energy due to the extra-ionic charge of the substrate increases by $-(0.25)\Delta X^2$ eV with the increase of ΔX.

The difference in electronegativity indicates the shift of the valence electron distribution from the center of the cation and the anion. The Coulomb interaction between the electrons shifted to the anion and the holes shifted to the cation produces the "extra-ionic" energy.[54] This extra-ionic energy dominates the lattice potential of the substrate. The contribution of the lattice potential to the photoemission initial-state effect of the Pd atom dissolved into the matrix of the substrate is greater for a more ionic substrate than that for a more covalent substrate. The greater the difference in electronegativity, the more ionic the bond is said to be, and the greater its heat of formation. We can know the difference in electronegativity of the substrate components from the change in the photoemission initial-state effect of the evaporated Pd with the coverage. It may also be possible to estimate the heat of formation and the bond ionicity of the substrate through the change in the photoemission initial-state effect of evaporated Pd.

V. CONCLUDING REMARKS

In this paper we presented the core-level photoelectron and core-valence-valence Auger electron studies of small Pd clusters supported on various substrates. The Pd $3d_{5/2}$ BE shifts positively as one goes from metallic Pd to small Pd clusters supported on substrate.

The photoemission initial-state effect is responsible for the Pd $3d_{5/2}$ BE shifts in small Pd clusters supported on the conductive amorphous carbon substrate. The photoemission final-state effect predominantly gives rise to the Pd $3d_{5/2}$ BE shifts in small Pd clusters supported on the insulative SiO_2 and Al_2O_3 substrates, which are expected to be weakly interacting with the cluster. The Pd $3d_{5/2}$ BE shifts in small Pd clusters supported on semiconducting InSb and InP substrates, which are expected to be

strongly interacting to the cluster, are primarily due to the photoemission initial-state effect. The role of photoemission final-state effect in the Pd $3d_{5/2}$ BE shifts increases with the increase of the Schottky barrier height of the semiconductor substrates and the bulk polarizability of the insulator substrates.

In the case of conductor and semiconductor substrates, fast electronic extra-atom relaxation can take place readily, therefore the conduction electrons of the substrates flow to the small Pd clusters for screening the incremental Pd core hole through the Schottky barrier. So, the ratio of the change in the core eigenvalue to the one-hole dynamic extra-atomic relaxation energy is larger for these substrates than that observed in the case of insulator substrates. In insulator substrates the mechanism of extra-atomic relaxation is the screening of positive charge by the polarization of the electronic charge on neighboring ions. The polarization energy of the highly polarizable substrate is smaller than that of less polarizable substrate. Therefore, the change of the one-hole dynamic extra-atomic relaxation energy observed in small Pd clusters on insulator substrates, which depends on the relative abilities of the polarizability of the substrate and the Pd metal, increases with the increase of the bulk polarizability of the substrate.

In the case of inert carbon substrate, the degree of charge transfer between the cluster and the substrate should be negligible in the time scale of photoemission, the Pd $3d_{5/2}$ BE shifts are due to photoemission initial-state effect.

This is consistent with Mason.[13] Mason proposed that the increase of core-level BE is due to the changes in the electronic configurations of the atoms in the cluster. The number of d electrons per metal atom in a small cluster is smaller than that in the bulk metal because of the intra-atomic sp-d rehybridization. The reduction in the compositions of the valence electrons in the Wigner-Seitz cell volume has been suggested as the reason for the increase in core-level BE in small clusters.[6] As one goes from small clusters to bulk metal, the Hartree-Fock potential experienced by the core electron may be altered because the valence electrons are compressed into Wigner-Seitz cell volume in bulk metal.[56] The compression increases the valence-electron—core-electron repulsion.

Cheung[18] reported a reduction in the line-shape asymmetry in small Pd clusters on carbon substrate. The reduction in the line asymmetry indicates the decrease in the electron-hole screening in small clusters. This means a corresponding reduction in the density of states $\rho(E_F)$ and/or in the screened core-hole potential v at the Fermi level.[57] This is consistent with the valence-band studies by photoemission[6,7,17,21] and quantum-mechanical calculations,[58] which indicate a decrease in $\rho(E_F)$ as the cluster size decreases. The reduction of v may be caused by the changes in the dielectric constant of the valence electrons. Ascarelli *et al.*[59] reported the increase of linewidth in a small Au particle with a decreasing particle's size. They have shown that the dielectric constant of a finite electron gas can be changed drastically when the size of the system is of the order of the Fermi-Thomas screening length.

Citrin and Wertheim[22] suggested that the positive core-level BE shift in small clusters relative to that of the bulk metal is mainly due to the difference in the choice of the reference level. There is a serious difficulty in their explanation. They assumed that small cluster has the same work function as that of the bulk. From classical electrostatics, we know that the work function of a metal sphere is larger than that of an infinite metal plane as mentioned in Sec. II. Thus, taking the vacuum level as the reference level, the cluster is expected to have a higher core-level BE than that of the bulk, assuming that initial states remain the same.

The change in the photoemission initial-state effect denotes the change of the potential energy of the Pd core electron for small Pd clusters on the substrate. The change in the term of core eigenvalue suggests that the extra-ionic energy of the substrate affects the core-electron potential of evaporated Pd atoms. The greater the difference in electronegativity of the substrate components, the larger its extra-ionic energy. The extra-ionic energy dominates the lattice potential of the ionically bonded substrate. The change in the photoemission initial-state effect of Pd is smaller for a more ionic substrate than that for a more covalent substrate. We can know the thermodynamic property of the substrate through the change in the photoemission initial-state effect of evaporated Pd.

We imply that initial-state effect is substantially important for the positive shifts of core-level electron BE in small Pd clusters on various substrates. The importance of the final-state effect is emphasized with the variation of the mechanism of extra-atomic relaxation in the substrate. We can know the thermodynamic property of the substrate through the change in the photoemission initial-state effect of evaporated Pd.

ACKNOWLEDGMENTS

The authors thank Miss K. Oki for assistance and Dr. T. Morimoto and Dr. F. Konishi for support of this work.

APPENDIX

In this appendix we discuss the influence of metal-semiconductor interface reaction on the Pd core-level-electron BE measurement.

Figure 8 shows the core-level-electron BE's of the InSb substrate components versus the Pd coverage. The In $3d_{5/2}$ BE remains constant and is identical to that obtained for InSb in the low-coverage region (less than 1×10^{15} atoms cm^{-2}). In the region of intermediate coverage [$(0.1-1)\times10^{16}$ atoms cm^{-2}] the In $3d_{5/2}$ BE decreases by 0.5 eV with increasing Pd coverage. The In $3d_{5/2}$ BE in the high-coverage region (more than 1×10^{16} atoms cm^{-2}) is constant.

The Sb $3d_{5/2}$ BE remains constant and is identical to that obtained for InSb in the low-coverage region (less than 3×10^{15} atoms cm^{-2}). In the region of intermediate-coverage [$(0.3-1)\times10^{16}$ atoms cm^{-2}] the Sb $3d_{5/2}$ BE increases by 0.6 eV with increasing Pd coverage. The Sb $3d_{5/2}$ BE in the high-coverage region (more than 1×10^{16} atoms cm^{-2}) is constant.

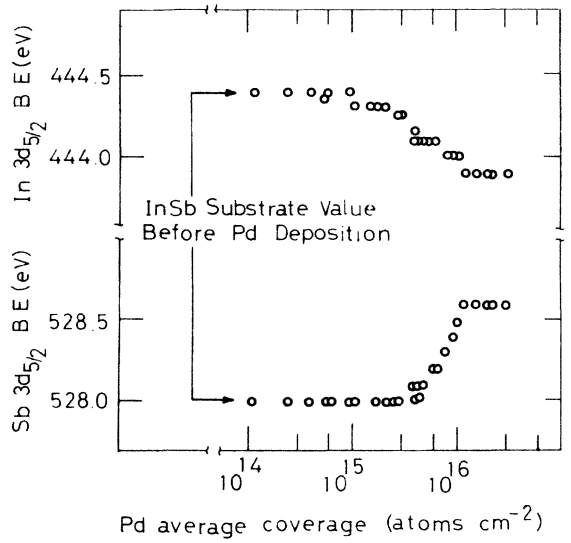

FIG. 8. Coverage dependence of the In $3d_{5/2}$ and Sb $3d_{5/2}$ electron binding energies (BE) of the InSb substrate.

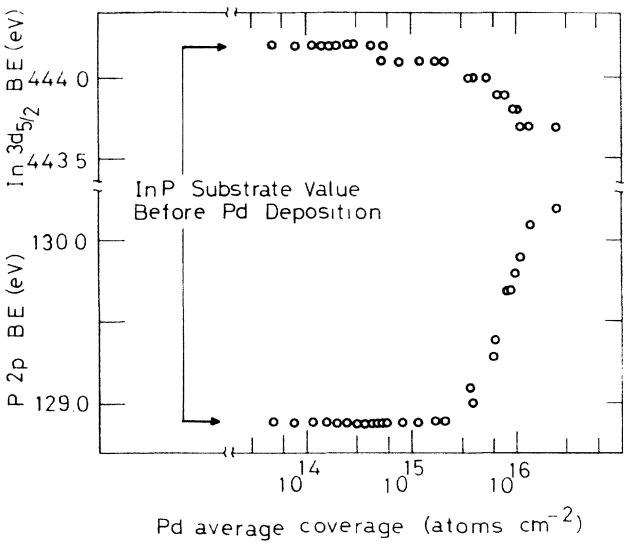

FIG. 9. Coverage dependence of the In $3d_{5/2}$ and P $2p$ electron binding energies (BE) of the InP substrate.

Figure 9 shows the core-level-electron BE's of the InP substrate components versus the Pd coverage. The In $3d_{5/2}$ BE remains constant and is identical to that obtained for InP in the low-coverage region (less than 8×10^{14} atoms cm^{-2}). In the region of intermediate coverage [(8×10^{14})—(1×10^{16}) atoms cm^{-2}] the In $3d_{5/2}$ BE decreases by 0.5 eV with increasing Pd coverage. The In $3d_{5/2}$ BE in the high-coverage region (more than 1×10^{16} atoms cm^{-2}) is constant.

The P $2p$ BE remains constant and is identical to that obtained for InP in the low-coverage region (less than 3×10^{15} atoms cm^{-2}). In the region of intermediate-coverage [$(0.3-1)\times10^{16}$ atoms cm^{-2}] the P $2p$ BE increases by 1.3 eV with increasing Pd coverage.

It is obvious that the core-level-electron BE's of the substrate components remain constant at Pd coverages below 1×10^{15} atoms cm^{-2}. The values of the BE's are identical to those obtained before Pd deposition. In the low-coverage region there is no evidence of the occurrence of the interface reaction or the formation of Pd-anion and Pd-cation compounds.

In the higher-coverage region (more than 1×10^{15} atoms cm^{-2}) the cation core-level-electron BE of the InSb and InP substrates decreases by 0.5 eV with increasing Pd coverage. The anion core-level-electron BE increases by 0.6 and 1.3 eV for the InSb and InP substrates, respectively. The interface reaction between the Pd clusters and the semiconductor substrates occurred in this coverage region (1—10 monolayers).

This result is consistent with other interface studies of metals on semiconductors showing that interdiffusion and interface reaction occurred and that metal-anion and metal-cation compounds formed.[60,61] The core-level-electron BE changes of the semiconductor substrate components observed in the higher-coverage region can be explained by the formation of Pd-anion and Pd-cation compounds. In the case of an InP substrate the In $3d_{5/2}$ BE shift in the higher-coverage region may be due to the formation of an In-Pd alloy.[61] This probably happened for InSb.

The chemical state of the freshly deposited Pd atoms in the surface of the clusters on the semiconductor dominates the information carried by the Pd $3d_{5/2}$ electron because the electron escape depth decays exponentially. We observe predominantly the top surface Pd atoms in the clusters where the interface reaction has not yet occurred. So, the interface reaction between the Pd and the semiconductors does not seriously flaw the results of the Pd cluster work on InP and InSb. The Pd $3d_{5/2}$ BE shifts observed in small Pd clusters supported on the semiconductor substrates are worthwhile to discuss the photoemission initial- and final-state effects.

[1]P. N. Ross, K. Kinoshita, and P. Stonehart, J. Catal. **32**, 163 (1974).
[2]S. Ladas, R. A. Dalla Betta, and M. Boudart, J. Catal. **53**, 356 (1978).
[3]J. C. Vedrine, M. Dufaux, C. Naccache, and B. Imelik, J. Chem. Soc. Faraday Trans. **74**, 440 (1978).
[4]H. Arai and T. Kunugi, J. Catal. **39**, 294 (1975).
[5]F. Bozon-Verdurax, A. Omar, J. Escard, and B. Pontvinne, J. Catal. **53**, 126 (1978).
[6]W. F. Egelhoff, Jr. and G. G. Tibbetts, Phys. Rev. B **19**, 5028 (1979).
[7]W. F. Egelhoff, Jr. and G. G. Tibbetts, Solid State Commun. **29**, 53 (1979).
[8]M. G. Mason and R. C. Baetzold, J. Chem. Phys. **64**, 271 (1976).
[9]G. Apai, S.-T. Lee, and M. G. Mason, Solid State Commun.

37, 213 (1981).
[10]H. Roulet, J.-M. Mariot, G. Dufour, and C. F. Hague, J. Phys. F **10**, 1025 (1980).
[11]L. Oberli, R. Monot, H. J. Mathieu, D. Landolt, and J. Buttet, Surf. Sci. **106**, 301 (1981).
[12]S.-T. Lee, G. Apai, M. G. Mason, R. Benbow, and Z. Z. Hurych, Phys. Rev. B **23**, 505 (1981).
[13]M. G. Mason, Phys. Rev. B **27**, 748 (1983).
[14]K. S. Liang, W. R. Salaneck, and I. A. Aksay, Solid State Commun. **19**, 329 (1976).
[15]S. Kohiki, Appl. Surf. Sci. **17**, 497 (1984); S. Kohiki and K. Oki, J. Electron Spectrosc. Relat. Phenom. **36**, 105 (1985); S. Kohiki, K. Oki, and F. Konishi, Anal. Sci. **1**, 115 (1985).
[16]G. K. Werthiem, S. B. Dicenzo, and S. E. Youngquist, Phys. Rev. Lett. **51**, 2310 (1983).
[17]M. G. Mason, L. J. Gerenser, and S.-T. Lee, Phys. Rev. Lett. **39**, 288 (1977).
[18]T. T. P. Cheung, Surf. Sci. **140**, 151 (1984).
[19]S. Kohiki, Appl. Surf. Sci. **25**, 81 (1986).
[20]R. Unwin and A. M. Bradshaw, Chem. Phys. Lett. **58**, 58 (1978).
[21]Y. Takasu, R. Unwin, B. Tesche, A. M. Bradshaw, and M. Grunze, Surf. Sci. **77**, 219 (1978).
[22]P. H. Citrin and G. K. Wertheim, Phys. Rev. B **27**, 3176 (1983).
[23]J. W. Gadzuk, in *Photoemission and The Electronic Properties of Surfaces,* edited by B. Feuerbacher, B. Fitton, and R. F. Willis (Wiley, Chichester, 1978).
[24]U. Gelius, Phys. Scr. **9**, 133 (1974).
[25]D. A. Shirley, J. Electron Spectrosc. Relat. Phenom. **5**, 135 (1974); Phys. Rev. A **7**, 1520 (1973); Chem. Phys. Lett. **17**, 312 (1972).
[26]L. Hedin and G. Johansson, J. Phys. B **2**, 1336 (1969).
[27]S. P. Kowalczyk, R. A. Pollak, F. R. McFeely, L. Ley, and D. A. Shirley, Phys. Rev. B **8**, 2387 (1973).
[28]W. N. Asaad and E. H. S. Burhop, Proc. Phys. Soc., London **71**, 369 (1958).
[29]E. U. Condon and G. H. Shortley, in *The Theory of Atomic Spectra* (Cambridge University Press, London, 1970).
[30]J. B. Mann, Los Alamos Scientific Laboratory Report No. LASL-3690, 1967 (unpublished).
[31]S. P. Kowalczyk, L. Ley, F. R. McFeely, R. A. Pollak, and D. A. Shirley, Phys. Rev. B **9**, 381 (1974).
[32]C. D. Wagner, Faraday Discuss. Chem. Soc. **60**, 291 (1975); C. D. Wagner, L. H. Gale, and R. H. Raymond, Anal. Chem. **51**, 466 (1979).
[33]F. Bechstedt, R. Enderlein, R. Fellenberg, P. Streubel, and A. Meisel, J. Electron Spectrosc. Relat. Phenom. **31**, 131 (1983).
[34]A. Schmidt-Ott, P. Schurtenberger, and H. C. Siegmann, Phys. Rev. Lett. **45**, 1284 (1980).
[35]D. M. Wood, Phys. Rev. Lett. **46**, 749 (1981).
[36]Strictly speaking, it is true only when there is sufficient electric contact between the analyzer and the clusters. If the clusters are isolated by a rare-gas layer of sufficient thickness to permit charge neutralization by tunneling from the substrate, the core-level-electron BE shows a systematic variation determined by the work function of the substrate. [M. Strongin, X. Pan, V. Murgai, S. Raaen, and P. H. Citrin, Bull. Am. Phys. Soc. **31**, 448 (1986).] This shows that clusters could be referenced to either the Fermi level or the vacuum level.
[37]S. Kohiki, T. Ohmura, and K. Kusao, J. Electron Spectrosc. Relat. Phenom. **28**, 229 (1983); **31**, 85 (1983).
[38]J. F. Hamilton and P. C. Logel, Thin Solid Films **23**, 89 (1974).
[39]K. Hübner, Phys. Status Solidi A **40**, 487 (1977); K. Hübner and A. Lehmann, *ibid.* **46**, 451 (1978).
[40]L. Ley, R. A. Pollack, F. R. McFeely, S. P. Kowalczyk, and D. A. Shirley, Phys. Rev. B **9**, 600 (1974).
[41]D. Pope, W. L. Smith, M. J. Eastlake, and R. L. Moss, J. Catal. **22**, 72 (1971); R. T. K. Baker, E. B. Prestridge, and R. L. Garten, *ibid.* **56**, 390 (1979).
[42]D. A. Shirley, in *Photoemission in Solids,* edited by M. Cardona and L. Ley (Springer, Berlin, 1978), Vol. 1, p. 177.
[43]C. S. Fadley, S. B. M. Hagstrom, M. P. Klein, and D. A. Shirley, J. Chem. Phys. **48**, 3779 (1968).
[44]B. Johansson and N. Mårtensson, Phys. Rev. B **21**, 4427 (1980); N. Mårtensson and B. Johansson, Solid State Commun. **32**, 791 (1979).
[45]P. Steiner, S. Hüfner, N. Mårtensson, and B. Johansson, Solid State Commun. **37**, 73 (1981).
[46]A. R. Miedema, J. Less-Common Met. **32**, 117 (1973); **46**, 67 (1976); Philips Tech. Rev. **36**, 217 (1976); Physica **100B**, 1 (1980); A. R. Miedema, R. Boom, and F. R. De Boer, J. Less-Common Met. **41**, 283 (1975); R. Boom, F. R. De Boer, and A. R. Miedema, *ibid.* **45**, 237 (1976); A. R. Miedema, F. R. De Boer, and R. Boom, CALPHAD: Comput. Coupling Phase Diagrams Thermochem. **1**, 341 (1977).
[47]W. Lambrecht, N. J. Castellani, and D. B. Leroy, J. Electron Spectrosc. Relat. Phenom. **37**, 87 (1985).
[48]N. Mårtensson, R. Nyholm, H. Calén, J. Hedman, and B. Johansson, Phys: Rev. B **24**, 1725 (1981).
[49]J. C. Phillips, *Bonds and Bands in Semiconductors* (Academic, New York, 1973).
[50]C. A. Mead and W. G. Spitzer, Phys. Rev. **134**, A713 (1964).
[51]C. A. Mead, Appl. Phys. Lett. **6**, 103 (1965).
[52]S. Kurtin, T. C. McGill, and C. A. Mead, Phys. Rev. Lett. **22**, 1433 (1969).
[53]K. Siegbahn, C. Nordling, G. Johansson, J. Hedman, P. F. Heden, K. Hamrin, U. Gelius, T. Bergmark, L. O. Werne, R. Manne, and Y. Baer, *ESCA Applied to Free Molecules* (Elsevier, Amsterdam, 1971); U. Gelius, Phys. Scr. **9**, 133 (1974).
[54]L. Pauling, *The Nature of the Chemical Bond* (Cornell University Press, Ithaca, NY, 1960).
[55]R. H. West and J. E. Castle, Surf. Int. Anal. **4**, 68 (1982).
[56]L. Hodges, R. E. Watson, and H. Ehrenreich, Phys. Rev. B **15**, 3953 (1972).
[57]The singularity index α is a measure of the asymmetry. Within the first Born approximation [J.J. Hopfield, Comments Solid State Phys. **11**, 40 (1969)], it can be expressed in terms of the density of states per unit volume $\rho(E_F)$ at the Fermi level and the screened potential of the core-level v: $\alpha=2[\rho(E_F)v]^2$.
[58]R. P. Messmer, S. K. Knudson, K. H. Johnson, J. B. Diamond, and C. Y. Yang, Phys. Rev. B **13**, 1396 (1976).
[59]P. Ascarelli, M. Cini, G. Missoni, and N. Nistico, J. Phys. (Paris) Colloq. **38**, C2-125 (1977).
[60]L. J. Brillson, C. F. Brucker, A. D. Katnani, N. G. Stoffel, R. Daniels, and G. Margaritondo, Surf. Sci. **132**, 212 (1983).
[61]T. Kendelewicz, N. Newman, R. S. List, I. Lindau, and W. E. Spicer, J. Vac. Sci. Technol. B **3**, 1206 (1985).